AGE (2013) 35:1219–1234
DOI 10.1007/s11357-012-9450-6

Western-style diet modulates contractile responses to phenylephrine differently in mesenteric arteries from senescence-accelerated prone (SAMP8) and resistant (SAMR1) mice

Francesc Jiménez-Altayó · Yara Onetti · Magda Heras · Ana P. Dantas · Elisabet Vila

Received: 14 March 2012 / Accepted: 24 June 2012 / Published online: 10 July 2012

Abstract The influence of two known cardiovascular risk factors, aging and consumption of a high-fat diet, on vascular mesenteric artery reactivity was examined in a mouse model of accelerated senescence (SAM). Five-month-old SAM prone (SAMP8) and resistant (SAMR1) female mice were fed a Western-type high-fat diet (WD; 8 weeks). Mesenteric arteries were dissected, and vascular reactivity, protein and messenger RNA expression, superoxide anion ($O_2^{\cdot-}$) and hydrogen peroxide formation were evaluated by wire myography, immunofluorescence, RT-qPCR, ethidium fluorescence and ferric-xylenol orange, respectively. Contraction to KCl and relaxation to acetylcholine remained unchanged irrespective of senescence and diet. Although similar contractions to phenylephrine were observed in SAMR1 and SAMP8, accelerated senescence was associated with decreased eNOS and nNOS and increased $O_2^{\cdot-}$ synthesis. Senescence-related alterations were compensated, at least partly, by the contribution of NO derived from iNOS and the enhanced endogenous antioxidant capacity of superoxide dismutase 1 to maintain vasoconstriction. Administration of a WD induced qualitatively different alterations in phenylephrine contractions of mesenteric arteries from SAMR1 and SAMP8. SAMR1 showed increased contractions partly as a result of decreased NO availability generated by decreased eNOS and nNOS and enhanced $O_2^{\cdot-}$ formation. In contrast, WD feeding in SAMP8 resulted in reduced contractions due to, at least in part, the increased functional participation of iNOS-derived NO. In conclusion, senescence-dependent intrinsic alterations during early stages of vascular senescence may promote vascular adaptation and predispose to further changes in response to high-fat intake, which may lead to the progression of aging-related cardiovascular disease, whereas young subjects lack the capacity for this adaptation.

Keywords Aging · Western diet · Nitric oxide · Oxidative stress · Endothelium

Ana P. Dantas and Elisabet Vila has equal contribution in senior authorship.

F. Jiménez-Altayó (✉) · Y. Onetti · E. Vila
Departament de Farmacologia, Terapèutica i Toxicologia,
Institut de Neurociències, Facultat de Medicina,
Universitat Autònoma de Barcelona (UAB),
08193 Bellaterra,
Cerdanyola del Vallès, Spain
e-mail: francesc.jimenez@uab.cat

M. Heras · A. P. Dantas
Institut Clínic del Tòrax, Institut d'Investigacions
Biomèdiques August Pi i Sunyer (IDIBAPS),
08036 Barcelona, Spain

Introduction

Aging of the cardiovascular system is a multifactorial process that involves changes at many different levels,

resulting in altered functioning and increased susceptibility to cardiovascular disease. The control of blood flow and pressure is critically influenced by vascular tone, which reflects the balance between constrictor and dilator influences (Barton 2010). Vascular tone can be regulated either by substances directly modulating the smooth muscle or by the indirect influence of the endothelium, which releases bioactive molecules that diffuse to the smooth muscle. Aging alters the contribution of these factors in vascular responses by generally reducing endothelial-mediated relaxation and increasing or decreasing contractile responses to several agonists (Briones et al. 2005a; Hausman et al. 2011; Marín and Rodriguez-Martínez 1999; Matz et al. 2000; Stewart et al. 2000; Van Guilder et al. 2007). One of these factors, aging-induced increase of reactive oxygen species (ROS) production, has been well described (Ungvari et al. 2008).

Several factors can potentially modify the impact of aging on the cardiovascular system. Weight gain is an independent risk factor for cardiovascular dysfunction and therefore is associated with an increased incidence of hypertension, stroke, diabetes and peripheral arterial disease (Hubert et al. 1983; Kannel et al. 1996). Experimental evidence suggests that mice fed a high-fat diet exhibit enhanced ROS production, impaired vascular relaxation and altered contractions (Barton 2010; Kobayasi et al. 2010; Matsumoto et al. 2006; Mundy et al. 2007; Rodriguez et al. 2006; Ungvari et al. 2010).

The similarities of the mechanisms activated by obesity and aging suggest that the former can be considered to have effects consistent with accelerated vascular aging (Barton 2010). This hypothesis may also lead to the proposition that the effects of aging and obesity could be additive on vascular responses, and thus dietary fat intake may possibly exacerbate the adverse effects of aging (Nakamura et al. 1989; Spagnoli et al. 1991). Nevertheless, several studies dealing with the effects on aging of high-fat feeding have produced contradictory results, and more prominent alterations in young than in old animals have also been reported (Cortes et al. 2002; Erdos et al. 2011). Therefore, the mechanisms by which weight gain can modify the outcome of cardiovascular aging are far from being well understood.

After the first report in 1981 by Takeda et al. (1981), numerous studies have demonstrated that senescence-accelerated mice (SAM) show age-associated alterations commonly found in aging humans. Compelling evidence indicates that several strains of the senescence-accelerated prone mice (SAMP), including SAMP8, show signs of accelerated senescence of the cardiovascular system (Han et al. 1998; Lauzier et al. 2008; Lloréns et al. 2007; Novella et al. 2010, 2011; Yagi et al. 1995; Zhu et al. 2001). Interestingly, increased contractility (Lloréns et al. 2007; Novella et al. 2010, 2011) and endothelial dysfunction (Lloréns et al. 2007; Novella et al. 2010) was observed in aortas from 6- to 7-month-old SAMP8 compared with SAMR1, an effect that could be partly attributed to elevated ROS production (Lauzier et al. 2008; Lloréns et al. 2007). Moreover, following administration of a high-fat diet, also known as Western diet (WD), more prevalent and extensive atherogenic lesions developed in aortas from SAMP8 than from SAMR1 (Fenton et al. 2004). Nevertheless, the role of accelerated senescence on small vessel reactivity and the impact of dietary fat intake have remained elusive. Novella et al. (2011) reported that vascular alterations begin earlier in SAMP8 and are manifest at an age of 6 months. The present study sought to determine the influence of accelerated senescence and high-fat intake on the reactivity of mesenteric arteries (MAs) from SAM at an early stage of vascular senescence and to investigate the mechanisms underlying those alterations, with special emphasis on the role of oxidative stress and changes in NO signaling.

Material and methods

Animals and diet

Female SAMR1 and SAMP8 mice were obtained from the breeding stock at Parc Científic de Barcelona, which began with matrices from Harlan (Harlan Laboratories UK, Bicester, UK), and housed according to institutional guidelines (constant room temperature at 22 °C, 12-h light/dark cycle, 60 % humidity and water ad libitum). Experiments were approved by the Ethics Committee of the Universitat de Barcelona and conformed to the US National Institutes of Health Guide for the Care and Use of Laboratory Animals. Both SAMR1 (n=48) and SAMP8 (n=47) were randomly separated at 5 months of age into two groups receiving ad libitum for 8 weeks the following: 1) a standard mice chow (control diet; Harlan Teklad mouse breeding and maintenance diet, Teklad Global

Diet-2018) and 2) a Western-type diet (Harlan Teklad Western Adjusted Calories Diet, TD.88137) (Fenton et al. 2004). Both diets were given as pellets, with the nutritional composition shown in Table 1.

Body weight was recorded at the beginning (5 months) and the end (7 months) of treatment, and average weight gain was calculated. Feed conversion efficiency was used as a measure of an animal's efficiency in converting feed mass into increased body mass. It was determined as the average mass of food intake (grams) divided by mass gain all over the dietary period. At 7 months old, all mice were anaesthetized with sodium pentobarbitone (40 mg/kg; i.p.) and decapitated. The mesenteric arcade was placed in cold physiological salt solution (PSS) of the following composition (in millimolar): NaCl 112.0, KCl 4.7, $CaCl_2$ 2.5, KH_2PO_4 1.1, $MgSO_4$ 1.2, $NaHCO_3$ 25.0 and glucose 11.1. At the day of sacrifice, fat accumulated within the abdominal cavity was carefully removed and weighed. Results were expressed as a function (percent) of total body weight. In some anaesthetized mice, blood samples (0.5 ml) were collected by cardiac puncture, and plasma was separated by centrifugation at 3000×*g*, 10 min, aliquoted and stored at −70 °C.

Table 1 Composition of experimental diets

	Control diet	Western diet
Ingredients (g/kg)		
Protein	186	173
DL-methionine	3	3
Carbohydrates	442	485
Cholesterol	ns	1.5
Mineral mix	39	35
Vitamin mix		
p-Aminobenzoic acid	0	0.10
Vitamin C	0	1
Biotin	0.0004	0.0005
Vitamin B12	0.00008	0.0003
Folic acid	0.0004	0.00002
Inositol	0.0014	0.0011
Vitamin K3	0.05	0.05
Niacin	0.07	0.10
Riboflavin	ns	0.02
Thiamin	ns	0.02
Vitamin A	0.015	0.04
Vitamin D	0.0015	0.004
Vitamin E	0.10	0.24
Antioxidant	ns	0.04
Nutritional composition (% by weight)		
Protein	18.6	17.3
Carbohydrate	44.2	48.5
Total fat	6.2	21.2
Saturated fat	0.9	13.3
Monounsaturated	1.3	5.9
Polyunsaturated	3.4	0.90
Cholesterol	ns	0.15

ns not specified

Tissue preparation

Segments of first-order branches [vascular reactivity, oil red O staining, superoxide anion ($O_2^{\cdot-}$) and hydrogen peroxide production and immunofluorescence] and first-, second- and third-order branches (RT-qPCR studies) of the superior MA were dissected free of fat and connective tissue in ice-cold PSS, maintained at 4 °C and gassed with 95 % O_2 and 5 % CO_2. The vessels were prepared essentially as previously described (Martínez-Revelles et al. 2012).

Wire myography

Reactivity was studied in vessels mounted on an isometric wire myograph (model 410 A; J.P. Trading, Aarhus, Denmark) filled with PSS (37 °C; 95 % O_2 and 5 % CO_2) following the protocol described previously (Martínez-Revelles et al. 2012). Optimal tension was assessed in preliminary experiments by subjecting arterial segments to different resting tensions and challenging with 100 mM KCl (Syyong et al. 2009). The optimal tension was the tension that resulted in the maximal force generated in response to 100 mM KCl, which was similar for SAMR1 and SAMP8 MAs (1.5 mN). Therefore, the vessels were stretched to 1.5 mN, washed and allowed to equilibrate for 30 min. The tissues were contracted three times with 100 mM KCl every 5 min until the amplitudes of the contractile responses were similar in magnitude. After washing, vessels were left to equilibrate for a further 30 min before starting the experiments.

Endothelial-dependent vasodilatations were studied by evaluating the relaxation induced by acetylcholine (ACh; 10^{-9} to 10^{-5} M) performed in 3×10^{-6} M phenylephrine (Phe)-precontracted vessels from SAMR1 and SAMP8. To investigate the influence of strain

and/or diet on contractile responses mediated by α_1-adrenoceptor stimulation, concentration–response curves to Phe (10^{-8} to 3×10^{-5} M) were performed. The effects of the nonselective nitric oxide synthase (NOS) inhibitor Nω-nitro-l-arginine methyl ester (L-NAME; 10^{-4} M), the selective iNOS inhibitor N-(3-(aminomethyl)benzyl)acetamidine hydrochloride (1400 W; 10^{-5} M) and the $O_2^{\cdot-}$ scavenger tempol (10^{-3} M) were determined by adding each treatment 30 min before Phe-induced contractions in vessels from both groups of mice.

Measurement of cholesterol levels

Plasma levels of total cholesterol were determined by a commercially fluorometric kit (Cayman Chemical, Ann Arbor, USA) following the manufacturer's directions.

Oil red O staining

Frozen transverse sections (14 μm) of MAs were placed on gelatin-coated slides and fixed with 3.7 % paraformaldehyde (PFA) for 1 h. After washing with phosphate buffer solution, sections were incubated for 30 min with 0.5 % oil red O. The vessels were then rinsed with distilled water and incubated with Gill's hematoxylin for 1 min. Colored and fluorescent images were captured with a microscope (Olimpus SX-31, ×40) using Soft Cell software.

Real-time quantitative RT-PCR

Messenger RNA (mRNA) expression of 1) the nitric oxide synthase isoforms (eNOS, iNOS and nNOS), 2) the subunits of NAD(P)H-oxidase (Nox-1, $p22^{phox}$ and $p47^{phox}$) and 3) the superoxide dismutase (SOD) isoforms [cytoplasmic Cu, Zn (SOD1), mitochondrial Mn (SOD2) and extracellular Cu, Zn (SOD3)] were quantified by Syber green-based quantitative real-time PCR as previously described (Caracuel et al. 2011; Márquez-Martín et al. 2012). Primer sequences for rodent genes used in this study are shown in Table 2. The 18 S ribosomal subunit of RNA was used as internal control (Applied Biosystem Inventoried Primer: Hs99999901 s1). RT-qPCR reactions were set following the manufacturer's conditions. Ct values obtained for each gene were referenced to r18S (ΔCt) and converted to the linear form using the term $2^{-\Delta Ct}$ as a value directly proportional to the copy number of complementary DNA and initial quantity of mRNA (Novensa et al. 2010).

Immunofluorescence

Frozen sections (14 μm) were incubated with primary antibodies as follows: mouse monoclonal anti-eNOS (1:100; BD Biosciences, Franklin Lakes, NJ, USA) or a rabbit polyclonal anti-iNOS (1:50; Thermo Scientific, Rockford, IL, USA), anti-nNOS (1:100; Life Technologies Ltd, Paisley, UK) and anti-nitrotyrosine (1:100; Merck Millipore, Billerica, MA, USA). Sections were processed for immunofluorescence staining essentially as previously described (Caracuel et al. 2011; Jiménez-Altayó et al. 2009; Martínez-Revelles et al. 2012). Quantitative analysis of fluorescence was performed with MetaMorph Image Analysis software (Molecular Devices, Sunnyvale, CA, USA). The fluorescence signal per area was measured in at least two rings of each animal, and the results were expressed as arbitrary units. All measurements were conducted blind.

Measurement of $O_2^{\cdot-}$ production

The oxidative fluorescent dye dihydroethidium, which in the presence of $O_2^{\cdot-}$ is oxidized to ethidium bromide, was used to evaluate production of $O_2^{\cdot-}$ in situ in frozen MA segments (14-μm thick), essentially as described previously (Jiménez-Altayó et al. 2009; Martínez-Revelles et al. 2012). Parallel sections were incubated with polyethylene glycol SOD (PEG-SOD; 500 U/ml) to evaluate the specificity of the signal. Quantitative analysis of $O_2^{\cdot-}$ production was performed with MetaMorph Image Analysis software (Molecular Devices, Sunnyvale, CA, USA). The fluorescence signal per area was measured in at least two rings of each animal, and the results were expressed as arbitrary units. All measurements were conducted blind.

Measurement of hydrogen peroxide production

Hydrogen peroxide formation was evaluated in the vascular wall by the ferric-xylenol orange hydroperoxide assay, adapted from a methodology previously described (Dantas et al. 2002; Hermes-Lima et al. 1995). This assay is based on the conversion of Fe^{+2} to Fe^{+3} at acidic pH in the presence of hydroperoxide, which in turn complexes with xylenol orange dye to

Table 2 Primer sequences for real-time quantitative RT-PCR

Rodent genes	Forward (5′-3′)	Reverse (5′-3′)
eNOS	TGTCACTATGGCAACCAGCGT	GCGCAATGTGAGTCCGAAAA
iNOS	TCAGCCACCTTGGTGAAGGGAC	TAGGCTACTCCGTGGAGTGAACA
nNOS	CAGCCGGTTCTTGCCCGGAGT	TGTCGCCGGCTTGGATAAGGC
Nox-1	CCTTCCATAAGCTGGTGGCAT	GCCATGGATCCCTAAGCAGAT
$p22^{phox}$	GGCCATTGCCAGTGTGATCTA	TGCTTGATGGTGCCTCCAA
$p47^{phox}$	AGGAGATGTTCCCCATTGAGG	CAGTCCCATGAGGCTGTTGAA
SOD1	ATGGCGACGAAGGCCGTGTG	GACCACCAGTGTGCGGCCAA
SOD2	TCCCAAGGGAAACACTCGGCT	AACCACTGGGTGACATCTACCAGAA
SOD3	GCGCTAACAGCCCAGGCTCCA	CTGTTCGGCTCGGTCGGGAA

yield a purple product. Briefly MA sections were initially incubated with 10 % methanol (v/v) for 20–30 min at room temperature, followed by incubation of reaction mixture containing 25 mM ammonium ferrous (II) sulfate, 2.5 M H_2SO_4, 4 mM butylhydroxytoluene and 125 μM xylenol orange in methanol. Colored images were captured with a microscope (Olimpus SX-31, ×40) using Soft Cell software. Quantitative analysis of hydrogen peroxide production was performed with Image J software. Percentage of labeled area was measured in at least two rings of each animal. All measurements were conducted blind.

Drugs

Drugs used were dihydroethidium, paraformaldehyde, phenylephrine hydrochloride, acetylcholine chloride, Nω-nitro-l-arginine methyl ester, N-(3-(aminomethyl)benzyl)acetamidine hydrochloride and tempol (Sigma-Aldrich). All drugs used for reactivity studies were dissolved in PSS.

Data analysis and statistics

Results are expressed as mean ± SEM of the number (n) of mice indicated in the figure legends. Vasoconstrictor responses were expressed as a percentage of the tone generated by 100 mM KCl. Vasodilator responses to ACh were expressed as a percentage of the previous tone generated by Phe. Area under the curve (AUC) was calculated from each individual concentration–response curve to ACh and Phe, and was expressed as arbitrary units. The dependence of vasoconstrictor and vasodilator response on strain and diet or on diet and vessel treatment was assessed by a two-way (strain/diet or diet/treatment) analysis of variance (ANOVA) with Bonferroni's post-test. Data analysis was carried out using GraphPad Prism v4. A value of $P<0.05$ was considered significant.

Results

General parameters

On control chow, all parameters were similar between strains, and WD increased weight gain, abdominal fat, feed conversion efficiency and cholesterol levels in both strains (Table 3). Nevertheless, WD intake did not result in the development of lipid lesions, measured in MAs from both groups by oil red O staining (data not shown).

Influence of senescence and diet on vascular reactivity

Contractile responses to KCl (100 mM) were similar irrespective of senescence (SAMR1 control: 0.59± 0.02 mN, n=38; SAMP8 control: 0.63±0.03 mN, n=48) and diet (SAMR1 WD: 0.60±0.03 mN, n=30; SAMP8 WD: 0.58±0.05 mN, n=25). Phe contracted endothelium intact MAs in a concentration-dependent manner (Fig. 1a). Although no senescence-associated difference was observed in either control group, high-fat diet induced opposite effects by either increasing ($P<0.01$) or decreasing ($P<0.05$) Phe contractions in SAMR1 and SAMP8, respectively (Fig. 1a). Conversely, neither senescence nor diet altered endothelium-dependent ACh-induced vasodilatation (Fig. 1b).

Table 3 Physiological and biochemical parameters in female SAMR1 and SAMP8

	SAMR1		SAMP8		*P* values			
	Control	WD	Control	WD	Control SAMR1/ SAMP8	Control/WD		WD SAMR1/ SAMP8
						SAMR1	SAMP8	
Initial body weight (g)	29.08±0.69	33.16±0.84	27.60±0.87	29.05±1.06	n.s.	0.01	n.s.	0.01
Weight gain (g)	2.28±0.30	4.82±0.36	1.64±0.42	6.15±0.86	n.s.	0.01	0.001	n.s.
Abdominal fat (% body weight)	4.47±0.51	8.32±0.65	4.40±0.50	9.75±0.69	n.s.	0.001	0.001	n.s.
Feed conversion efficiency (arbitrary units)	0.63±0.08	1.30±0.10	0.55±0.14	1.62±0.23	n.s.	0.01	0.001	n.s.
Cholesterol (mg/dl)	67.44±6.00	88.32±1.34	60.48±3.07	91.10±1.73	n.s.	0.001	0.001	n.s.

Results are the mean ± SEM from SAMR1 (control 22; WD 26) and SAMP8 (control 21; WD 26) mice. Two-way ANOVA with Bonferroni's post-test

WD Western diet, *n.s.* statistically nonsignificant

Influence of senescence and diet on NO-mediated responses

The nonselective NO synthase inhibitor L-NAME (10^{-4} M) enhanced the concentration–response curve to Phe in SAMR1 on control diet but not on WD (Fig. 2a). Nevertheless, in SAMP8 mice, vasoconstrictor responses to Phe after L-NAME were greater in both control-fed and WD mice (Fig. 2b). Treatment with 1400 W (10^{-5} M), a selective iNOS inhibitor, had no effect on diet-mediated changes in SAMR1 (Fig. 2c). Nevertheless, in SAMP8 mice, 1400 W reversed the WD-induced impairment of Phe contractions (Fig. 2d), but only induced a slight increase ($P<0.05$) on the maximum contraction (control: 180±6 % KCl, $n=16$; control+1400 W: 205±10 % KCl, $n=7$) on control diet.

Immunofluorescence and RT-qPCR studies revealed low levels of eNOS protein and mRNA

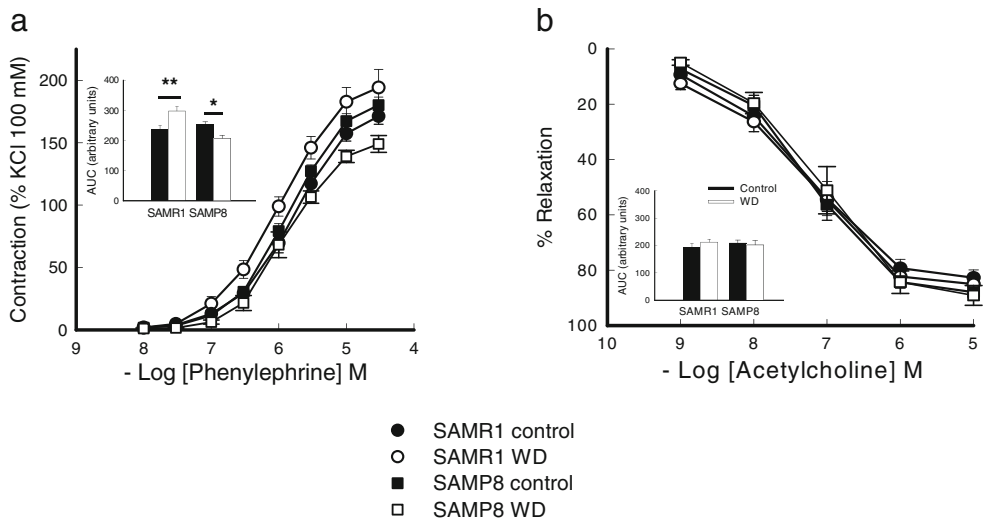

Fig. 1 Influence of senescence and diet on the concentration–response curve to phenylephrine (**a**) and acetylcholine (**b**) in mesenteric arteries from female SAMR1 and SAMP8 mice. *WD* Western diet. Results are the mean ± SEM from SAMR1 (control 16–20; WD 10–14) and SAMP8 (control 14–16; WD 7–10) mice. *$P<0.05$, **$P<0.01$ by two-way ANOVA with Bonferroni's post-test

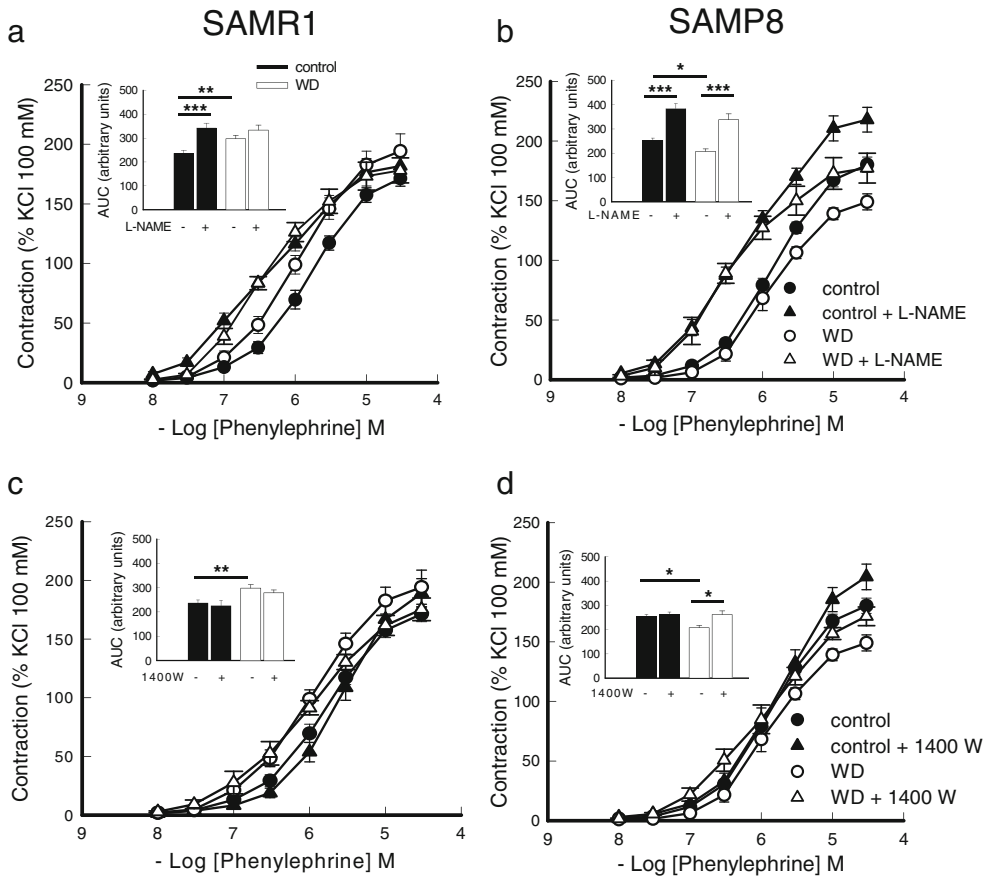

Fig. 2 Influence of senescence and diet on the concentration–response curve to phenylephrine in mesenteric arteries from female SAMR1 and SAMP8 mice. The role of eNOS and iNOS was assessed with L-NAME (100 μM) (**a**, **b**) or 1400 W (10 μM) (**c**, **d**). *WD* Western diet. Results are the mean ± SEM from SAMR1 (control 6–16; WD 4–10) and SAMP8 (control 5–14; WD 5–7) mice. *$P<0.05$, **$P<0.01$, ***$P<0.001$ by two-way ANOVA with Bonferroni's post-test

expression in SAMP8 and WD-fed mice (Fig. 3a, b). iNOS protein expression was similar in all vessels (Fig. 3a). However, quantitative analysis of iNOS mRNA showed greater levels ($P<0.05$) in SAMP8 compared to SAMR1 on both control diet and WD (Fig. 3b). nNOS protein expression was decreased ($P<0.01$) by senescence (Fig. 3a). WD intake either decreased ($P<0.05$) or increased ($P<0.05$) nNOS protein expression in SAMR1 and SAMP8, respectively (Fig. 3a). However, nNOS mRNA levels were enhanced in SAMP8 compared to SAMR1 irrespective of diet (Fig. 3b).

Influence of senescence and diet on oxidative stress

To determine the participation of $O_2^{\cdot-}$ on Phe-induced contractions during senescence and WD, vessels were incubated with the SOD mimetic tempol (10^{-3} M; Fig. 4). Tempol did not elicit any effect on Phe contractions in the two groups of mice on control diet. However, on WD-fed mice, treatment with tempol eliminated the WD-induced potentiation of Phe contractions in SAMR1 (Fig. 4a). Conversely, tempol had no significant effect on Phe contractions in SAMP8 on WD (Fig. 4b).

A slight fluorescence by ethidium bromide was observed along the vascular wall of SAMR1 and SAMP8 (Fig. 5a). WD augmented ($P<0.05$) the fluorescence in all three layers of the SAMR1 vessel wall, but did not change the fluorescence in SAMP8 (Fig. 5a), suggesting an increase in $O_2^{\cdot-}$ production after exposure to WD only in SAMR1. Weak fluorescence for nitrotyrosine was found on MA from SAMR1 on control diet (Fig. 5b). However, a marked

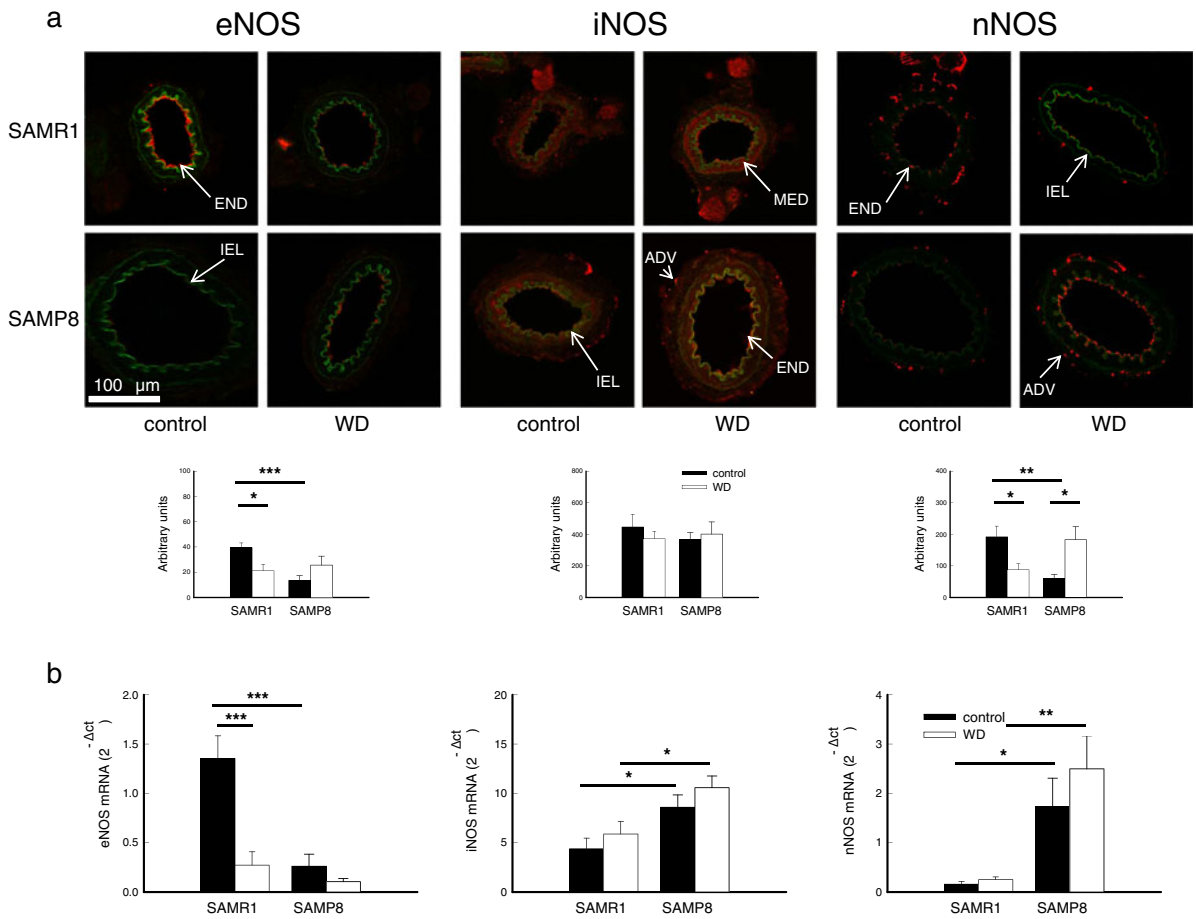

Fig. 3 Influence of senescence and diet on NOS expression in mesenteric arteries from female SAMR1 and SAMP8 mice. **a** Representative photomicrographs and quantification of eNOS, iNOS and nNOS immunofluorescence of confocal microscopic artery sections. Immunofluorescent signal (*red*) and natural autofluorescence of elastin (*green*) are shown. *ADV* adventitial layer, *END* endothelial layer, *MED* media layer, *IEL* internal elastic lamina, *WD* Western diet. Image size 238×238 µm. SAMR1 (control 5–6; WD 4–5) and SAMP8 (control 5–7; WD 4–5) mice. *$P<0.05$, **$P<0.01$, ***$P<0.001$ by two-way ANOVA with Bonferroni's post-test. **b** Comparative analysis of mRNA levels of eNOS, iNOS and nNOS in mesenteric arteries from female SAMR1 and SAMP8 mice. mRNA levels are expressed as $2^{-\Delta Ct}$ using 18 S as internal control. Results are the mean ± SEM from SAMR1 (control 6; WD 6) and SAMP8 (control 6; WD 6) mice. *$P<0.05$, **$P<0.01$, ***$P<0.001$ by two-way ANOVA with Bonferroni's post-test

increase ($P<0.01$) in nitrotyrosine immunofluorescence was observed in SAMP8 on control diet, suggesting a senescence-induced increase in peroxynitrite formation (Fig. 5b). WD increased ($P<0.05$) nitrotyrosine-induced fluorescence in SAMR1, but reduced ($P<0.01$) the fluorescence in SAMP8, indicating an increase or decrease, respectively, in peroxynitrite formation after exposure to WD (Fig. 5b). Quantitative analysis of mRNA levels of NAD(P)H-oxidase subunits (major source of vascular $O_2^{\cdot-}$) shows that Nox-1, $p22^{phox}$ and $p47^{phox}$ were expressed in MAs from both SAMR1 and SAMP8 (Fig. 5c). mRNA levels of Nox-1 ($P<0.01$) and $p22^{phox}$ ($P<0.05$) were significantly greater in SAMP8 compared to SAMR1 on control diet (Fig. 5c). Feeding animals a WD increased ($P<0.05$) mRNA levels of Nox-1, $p22^{phox}$ and $p47^{phox}$ in SAMR1 (Fig. 5c). In SAMP8, however, WD significantly increased ($P<0.01$) mRNA levels of $p47^{phox}$ without modifying those of Nox-1 and $p22^{phox}$ (Fig. 5c).

A slight hydrogen peroxide production was observed along the vascular wall of SAMR1 irrespective of diet (Fig. 6a). However, an increase in hydrogen peroxide production was observed in SAMP8 irrespective of diet (Fig. 6a). Quantitative analysis of

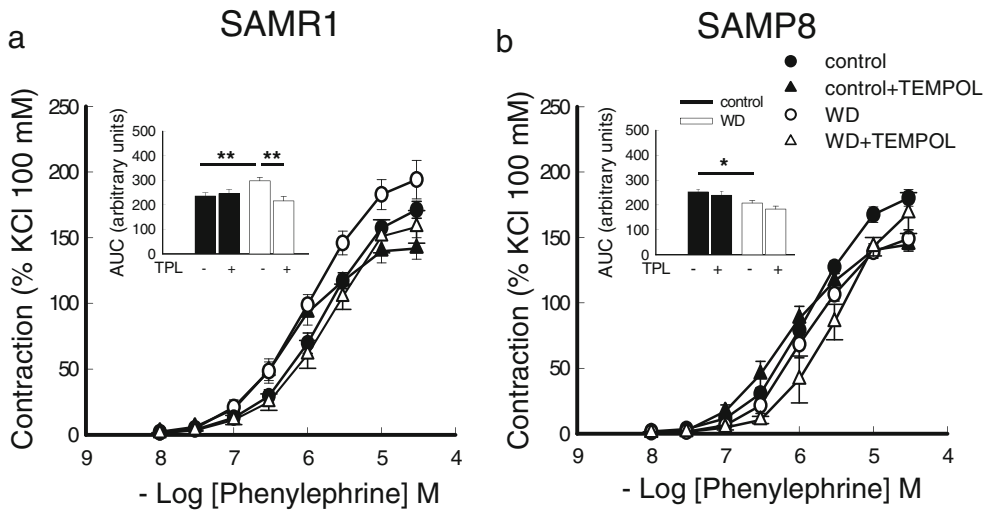

Fig. 4 Influence of senescence and diet on the concentration–response curve to phenylephrine in mesenteric arteries from female SAMR1 (**a**) and SAMP8 (**b**) mice. The role of superoxide anion was assessed with tempol (1 mM). *WD* Western diet. Results are the mean ± SEM from SAMR1 (control 4–16; WD 5–10) and SAMP8 (control 8–14; WD 3–7) mice. *$P<0.05$, **$P<0.01$ by two-way ANOVA with Bonferroni's post-test

mRNA levels of SOD shows that only SOD1 and SOD3 were prominently detected in MAs from both strains (Fig. 6b). mRNA levels of SOD1 were greater ($P<0.01$) in SAMP8 compared to SAMR1 either on control or WD (Fig. 6b). However, neither senescence nor diet modified mRNA levels of SOD3 (Fig. 6b).

Discussion

The present study shows similar vascular reactivity in MAs from SAMR1 and SAMP8, though marked changes at molecular levels are observed at an early stage of vascular senescence, suggesting a potential adaptive mechanism of blood vessels during the beginning of senescence. Furthermore, MAs from SAMR1 and SAMP8 are sensitive to functionally distinct changes in response to modifications in dietary fat intake. In this regard, the decreased reactivity observed in SAMP8 in response to high-fat feeding might constitute a counteractive adaptive mechanism, whereas the increased vascular reactivity in SAMR1 indicates a lack of capacity to adapt. Nevertheless, even though these vascular adaptations in SAMP8 might seem beneficial at this stage, it could lead to vascular injury (Moncada and Higgs 2006; Van der Loo et al. 2000) and hemodynamic decompensation (Gómez-Jiménez et al. 1995; Hollenberg et al. 2000).

The SAM model was chosen because the animals age fast and predictably without vascular damage at an early age (Butterfield and Poon 2005; Novella et al. 2010). Novella et al. (2011) identified the time points for some vascular functional and molecular changes in SAM and reported that although aging similarly affects aortic function in both SAMR1 and SAMP8, vascular alterations occur earlier in aorta from SAMP8 and are manifest at an age of 6 months. Therefore, we decided to begin treatment at 5 months and analyze vascular responses at 7 months of age in both SAMR1 and SAMP8, a period that coincides with the beginning of manifest vascular senescence in SAMP8. Importantly, SAM exhibits a diet-induced weight gain that is paralleled by augmented abdominal adiposity in a similar way to what occurs in humans. Despite that, SAMP8 did not differ from SAMR1 in weight gain and abdominal fat deposition on WD, and therefore we could exclusively establish the role of senescence on WD-induced effects. A previous study using this mice model established that aortas from SAMP8 are more prone than SAMR1 to early atherogenesis induced by WD (Fenton et al. 2004). Conversely, our studies showed no fatty lesion following WD in small arteries in both SAMR1 and SAMP8 mice.

In the present study, MA contractions to KCl and Phe were similar in SAMR1 and SAMP8 on control diet. The major novelty of the current study is that

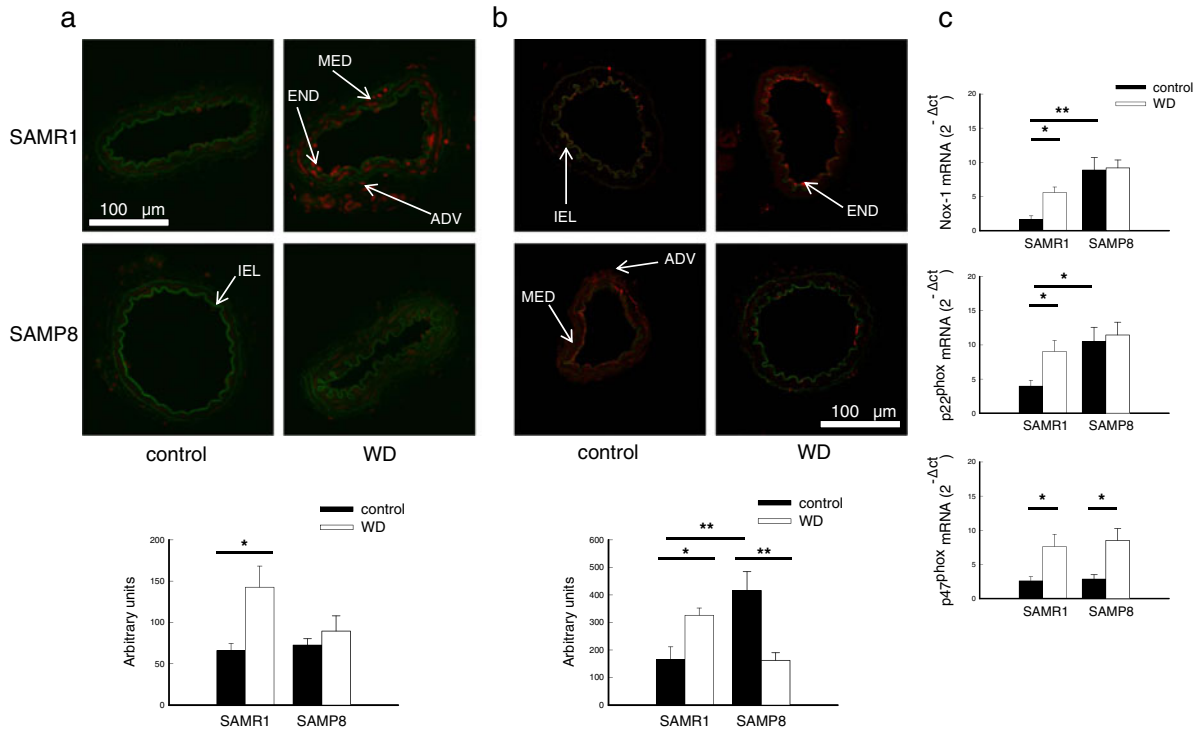

Fig. 5 Influence of senescence and diet on superoxide anion formation in mesenteric arteries from female SAMR1 and SAMP8 mice. **a** Representative photomicrographs and quantification of fluorescence of confocal microscopic artery sections labeled with the oxidative dye dihydroethidium, which produces a red fluorescence when oxidized to ethidium bromide by superoxide anion. Natural autofluorescence of elastin (*green*) is also shown. *ADV* adventitial layer, *END* endothelial layer, *MED* media layer, *IEL* internal elastic lamina, *WD* Western diet. Image size 238×238 µm. Results are the mean ± SEM from SAMR1 (control 5; WD 5) and SAMP8 (control 5; WD 5) mice. **P*<0.05 by two-way ANOVA with Bonferroni's post-test. **b** Representative photomicrographs and quantification of nitrotyrosine immunofluorescence of confocal microscopic artery sections. Immunofluorescent signal (*red*) and natural autofluorescence of elastin (*green*) are shown. *ADV* adventitial layer, *END* endothelial layer, *MED* media layer, *IEL* internal elastic lamina, *WD* Western diet. Image size 238×238 µm. SAMR1 (control 5; WD 5) and SAMP8 (control 5; WD 5) mice. **P*< 0.05, ***P*<0.01 by two-way ANOVA with Bonferroni's post-test. **c** Comparative analysis of mRNA levels of the NAD(P)H oxidase subunit Nox-1, $p22^{phox}$ and $p47^{phox}$. mRNA levels are expressed as $2^{-\Delta Ct}$ using 18 S as internal control. Results are the mean ± SEM from SAMR1 (control 6; WD 6) and SAMP8 (control 6; WD 6) mice. **P*<0.05, ***P*<0.01 by two-way ANOVA with Bonferroni's post-test

switching from standard chow to a high-fat diet alters the contractions to Phe in opposite directions in SAMR1 and SAMP8. Contractions to KCl were not modified by WD, which clearly shows that the observed differences on Phe contractions cannot be considered a generalized effect on smooth muscle contractility. Administration of a high-fat diet per se has yielded mixed results in the literature, and enhanced (Matsumoto et al. 2006) or unchanged (Eichhorn et al. 2009) Phe contractions of MAs from young mice have been reported. Interestingly, we observed that WD feeding enhanced Phe contractions in SAMR1, while it reduced such responses in SAMP8. It is worth mentioning that in both strains 8 weeks of high-fat consumption, leading to 7 % (SAMR1) and 15 % (SAMP8) increase in body weight over that observed in the control groups, was enough to promote such significant and qualitatively different alterations in vascular responses.

Altered small artery reactivity in disease is at least partly associated with changes in NO bioavailability (Vila and Salaices 2005). Therefore, alterations in the synthesis and/or effect of NO might explain the difference in Phe contractions induced by WD feeding. Phe responses were equally potentiated by L-NAME treatment in both groups on control diet, indicating a similar inhibitory role for NO on the modulation of

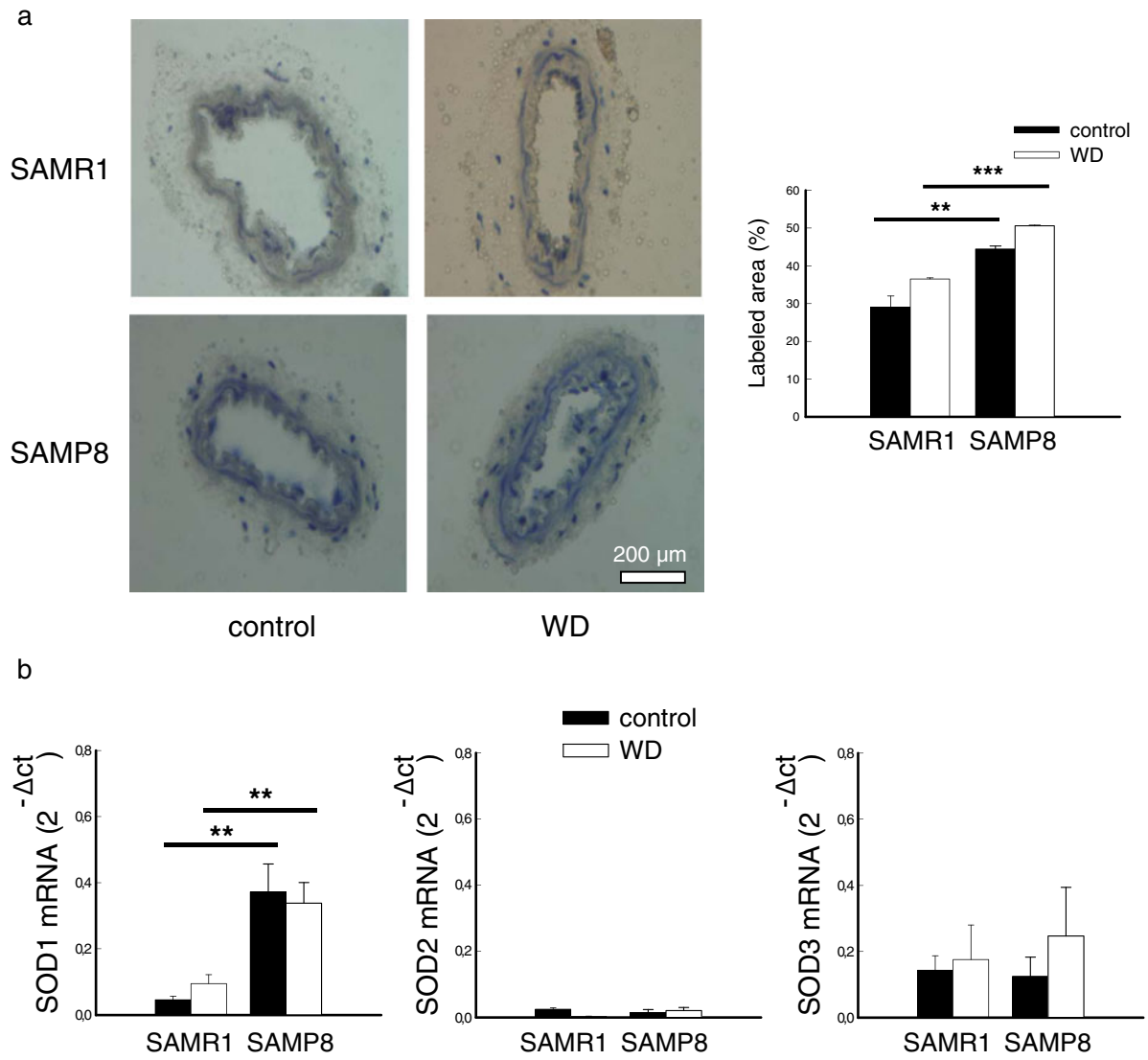

Fig. 6 Influence of senescence and diet on endogenous antioxidant capacity in mesenteric arteries from female SAMR1 and SAMP8 mice. **a** Representative photomicrographs and quantification of staining of microscopic artery sections. This assay is based on the conversion of Fe^{+2} to Fe^{+3} in the presence of hydroperoxide, which in turn complexes with xylenol orange dye to yield a purple product. *WD* Western diet. Image size 858×858 µm. Results are the mean ± SEM from SAMR1 (control 5; WD 7) and SAMP8 (control 8; WD 11) mice. $^{**}P<0.01$, $^{***}P<0.001$ by two-way ANOVA with Bonferroni's post-test. **b** Comparative analysis of mRNA levels of SOD1, SOD2 and SOD3. mRNA levels are expressed as $2^{-\Delta Ct}$ using 18 S as internal control. Results are the mean ± SEM from SAMR1 (control 6; WD 6) and SAMP8 (control 6; WD 6) mice. $^{**}P<0.01$ by two-way ANOVA with Bonferroni's post-test

Phe-induced MA contractions (Dora et al. 2000; Matsumoto et al. 2004) in SAMR1 and SAMP8. However, after high-fat diet feeding, suppression of the NO-mediated modulation of Phe contraction by L-NAME was seen only in SAMR1, suggesting a decreased NO production by WD only in those animals. Curiously, we observed eNOS protein and mRNA down-regulation not only in SAMR1 on WD, but also in SAMP8 on either control diet or WD. Those results agree with the observed lack of potentiation of Phe responses after exposure to L-NAME in SAMR1 on WD, but they are somewhat surprising given the observed potentiation of Phe contractions by L-NAME in SAMP8 irrespective of diet. These results led us to

speculate that in SAMP8 NO derived from other forms of NOS may overcome eNOS deficiency to maintain NO production.

In the vasculature, although eNOS is the primary source of NO under physiological conditions, NO derived from iNOS and nNOS may also play an important role under various pathological conditions (Chatterjee et al. 2008; Morishita et al. 2002; Yogo et al. 2000). Contrasting results regarding the influence of age on NOS expression have been reported (Briones et al. 2005a, 2005b; Piech et al. 2003; Yang et al. 2009; Zanetti et al. 2010). In the present study, in spite of higher mRNA levels of iNOS detected in SAMP8, protein expression was similar in MAs from SAMP8 compared to SAMR1. However, the inhibition of iNOS with 1400 W revealed an influence of NO from iNOS on Phe-induced contractions that was greater in WD than in control SAMP8 mice. We next established a potential role of nNOS for aging-associated NO production. Due to the lack of specific nNOS inhibitors, its contribution was determined through changes in protein and mRNA expression. Analysis of protein expression showed that nNOS was constitutively expressed in MAs from SAMR1 and decreased by senescence. Feeding a WD reduced nNOS expression in SAMR1 while enhanced its expression in SAMP8. On the other hand, we observed enhanced mRNA levels of nNOS in MAs from SAMP8 compared to SAMR1 irrespective of diet. It is worth mentioning that iNOS and nNOS transcription did not always recapitulate their protein expression. More likely, changes in translational mechanisms of this NOS isoforms would contribute to these effects. Together, these lines of evidence support the contribution of NO derived from iNOS as a compensatory mechanism to preserve the production of NO in the face of a decrease in the participation of other forms of NOS in early stages of vascular senescence. The potential contribution of NO derived from nNOS after feeding a WD in senescent mice cannot be discarded.

Although changes in NOS expression could explain the senescence- and diet-induced effects on vascular reactivity, the participation of ROS should also be considered, as aging and obesity are commonly associated with increases in ROS production (Barton 2010). The newly formed $O_2^{\cdot-}$ can scavenge NO reducing its bioavailability, thereby leading to vascular dysfunction (Hamilton et al. 2002). In our study, a marked increase in mRNA levels for NAD(P)H-oxidase subunits Nox-1, $p22^{phox}$ and $p47^{phox}$ as well as $O_2^{\cdot-}$ and nitrotyrosine formation was observed in MAs from SAMR1 receiving the WD, as already reported in young mice fed a high-fat diet (Eichhorn et al. 2009; Matsumoto et al. 2006). Based on these findings, we suggest that an increase in NO breakdown induced by an excess of $O_2^{\cdot-}$ could also play a role in the increased Phe contractions observed after WD feeding in SAMR1. The fact that the $O_2^{\cdot-}$ scavenger tempol abolished the enhancement of Phe contractions induced by WD in SAMR1 supports this hypothesis. However, vascular tone is influenced, among others, by various cyclooxygenase-derived products that may modulate vascular contractions with age (Novella et al. 2011). Several studies also indicate that obesity is associated with activation of cyclooxygenase-dependent vasoconstrictor pathways (Rask-Madsen and King 2007; Traupe et al. 2002). Therefore, the participation of additional factors in Phe-enhanced contractions in SAMR1 cannot be excluded. It should be noted that decreased NO availability in SAMR1 after WD feeding was not accompanied by impairment of endothelium-dependent relaxation to acetylcholine. Although we do not have a clear explanation for the lack of differences in acetylcholine-induced vasodilatation, we suggest that enhanced NO-independent relaxation might compensate for the loss of NO after WD feeding in SAMR1, as already described by others (Chadha et al. 2010). Further examination of the mechanisms involved in that preservation of endothelium-dependent relaxation is beyond the scope of the present study.

Interestingly, we did not find significant differences in $O_2^{\cdot-}$ formation between SAMR1 and SAMP8 fed control chow in spite of enhanced Nox-1 and $p22^{phox}$ mRNA levels in the latter. Similarly, after WD feeding, mRNA levels of Nox-1, $p22^{phox}$ and $p47^{phox}$ were comparable in SAMP8 and SAMR1, whereas $O_2^{\cdot-}$ formation along the MA wall was only enhanced in SAMR1. Consistent with these discrepancies, tempol diminished Phe-induced contractions in SAMR1 on WD, but it did not modify those in SAMP8 on either diet. We found increased nitrotyrosine formation in MA from SAMP8 on control diet. Thus, we cannot discard that increased iNOS-derived NO could at least partially account for unaltered $O_2^{\cdot-}$ formation in senescent mice despite increased NAD(P)H-oxidase expression. However, nitrotyrosine formation was, in

fact, decreased in MAs from SAMP8 on WD. We pursued further investigation to determine if the lack of $O_2^{\cdot-}$ formation in SAMP8 could also be a consequence of differences on endogenous SOD activity. Thus, we observed enhanced H_2O_2 formation and mRNA levels of SOD1 in vessels from SAMP8 on control diet and WD, suggesting that increased endogenous SOD1 antioxidant capacity may participate in buffering oxidative stress in SAMP8. Those results contrast with the aging-induced decline in SOD activity (Herrera et al. 2010), but reinforce the hypothesis that early stages of senescence are associated with the appearance of compensatory mechanisms. Adaptation of blood vessels has an essential putative role in protecting the vasculature against disease, but what really matters is the net balance between adaptation and injury (Ferrini et al. 2004). Thus, a prolonged activation of adaptive pathways may also be noxious and might ultimately lead to hemodynamic disturbances at later stages, exacerbating vascular injury (Gómez-Jiménez et al. 1995; Hollenberg et al. 2000). In addition, the observed vascular adaptation involves iNOS-derived NO that may act by itself as a cytotoxic agent (Moncada and Higgs 2006) and peroxynitrite, a potent harmful molecule that plays a role in vascular injury (Van der Loo et al. 2000). Conversely, the predisposition to increased reactivity upon high-fat intake reflects lack of adaptation in SAMR1 and might shed light on the mechanisms by which excessive weight gain during youth is a determinant of adult cardiovascular risk (Reilly and Kelly 2011; Sinaiko et al. 1999). However, this hypothesis remains to be fully elucidated.

Collectively, the present study shows that the lack of differences between SAMR1 and SAMP8 in Phe responses of MAs is a consequence of senescence-related changes at the molecular level. Thus, the observed down-regulation of eNOS and nNOS and up-regulation of $O_2^{\cdot-}$ synthesis in SAMP8 is compensated for, at least in part, by the contribution of NO derived from iNOS and the increased endogenous antioxidant capacity of SOD1 to maintain vasoconstriction. However, consumption of a high-fat diet induced qualitatively different alterations in Phe contractions of MAs from SAMR1 and SAMP8. SAMR1 showed increased contractions partly as a result of decreased NO availability generated by decreased eNOS and nNOS expression and enhanced $O_2^{\cdot-}$ formation. In contrast, high-fat feeding in SAMP8 resulted in reduced contractions due, at least in part, to the increased functional participation of NO derived from iNOS. Therefore, senescence-dependent intrinsic alterations during early stages of vascular senescence may promote adaptation and predispose to further changes in response to high-fat intake, which may be involved in the progression of aging-related cardiovascular disease. Certainly, the increase in the average age of the population will be one of the major medical and socioeconomic problems in the twenty-first century, and thus it is essential to understand the factors and mechanisms involved in the pathogenesis of aging. Our study emphasizes the need to investigate the effect of high-fat diet intake on vascular responses at different stages of aging to gain further understanding of their functional impact on the human vasculature.

Study limitation and future directions

Our aim was to evaluate the mechanisms of early vascular dysfunction induced by high-fat diet, commonly known as Western-type diet, and to determine if these changes occur similarly in the vasculature of SAMR1 and SAMP8. Our findings provide new insights on how short-term high-fat intake might affect small vessel function in young and aged individuals. Nevertheless, we are aware that our experimental condition may not reflect real-life situation, where the ingestion of high-fat diets generally occur over longer periods of time. Thus, our study provide no information on whether the observed effects are worsen or modified at long term, or yet, if they can be reversed by changing diet. Being a subject of great clinical relevance in modern society, long-term effects of high-fat intake and the mechanisms responsible to regulate vascular function during aging should be carefully pursued in an entirely new project.

Acknowledgments This work was financially supported by grants from the Ministerio de Ciencia e Innovación (SAF2010-19282), Instituto Carlos III (FIS PI080176; Red HERACLES RD06/0009) and Generalitat de Catalunya (2009SGR-890). Yara Onetti was supported by the Ministerio de Educación y Ciencia (FPI); Ana Paula Dantas was supported by a Miguel Servet fellowship from Ministerio de Sanidad, Servicios Sociales e Igualdad (CP06/00308). We acknowledge the confocal microscopy core from Universitat Autònoma de Barcelona. The authors are grateful to Nadia Castillo for the excellent technical assistance and appreciate the review of English grammar and usage by Elaine Lilly, Ph.D. (Writer's First Aid).

References

Barton M (2010) Obesity and aging: determinants of endothelial cell dysfunction and atherosclerosis. Pflugers Arch 460:825–837

Briones AM, Montoya N, Giraldo J, Vila E (2005a) Ageing affects nitric oxide synthase, cyclooxygenase and oxidative stress enzymes expression differently in mesenteric resistance arteries. Auton Autacoid Pharmacol 25:155–162

Briones AM, Salaices M, Vila E (2005b) Ageing alters the production of nitric oxide and prostanoids after IL-1beta exposure in mesenteric resistance arteries. Mech Ageing Dev 126:710–721

Butterfield DA, Poon HF (2005) The senescence-accelerated prone mouse (SAMP8): a model of age-related cognitive decline with relevance to alterations of the gene expression and protein abnormalities in Alzheimer's disease. Exp Gerontol 40:774–783

Caracuel L, Jiménez-Altayó F, Romo M, Márquez-Martín A, Dantas AP, Vila E (2011) Transient mesenteric ischemia leads to remodeling of rat mesenteric resistance arteries. Front Physiol 2:118

Chadha PS, Haddock RE, Howitt L, Morris MJ, Murphy TV, Grayson TH, Sandow SL (2010) Obesity up-regulates intermediate conductance calcium-activated potassium channels and myoendothelial gap junctions to maintain endothelial vasodilator function. J Pharmacol Exp Ther 335:284–293

Chatterjee A, Black SM, Catravas JD (2008) Endothelial nitric oxide (NO) and its pathophysiologic regulation. Vasc Pharmacol 49:134–140

Cortes MJ, Diez-Juan A, Perez P, Perez-Roger I, Arroyo-Pellicer R, Andres V (2002) Increased early atherogenesis in young versus old hypercholesterolemic rabbits by a mechanism independent of arterial cell proliferation. FEBS Lett 522:99–103

Dantas AP, Tostes RC, Fortes ZB, Costa SG, Nigro D, Carvalho MH (2002) In vivo evidence for antioxidant potential of estrogen in microvessels of female spontaneously hypertensive rats. Hypertension 39:405–411

Dora KA, Hinton JM, Walker SD, Garland CJ (2000) An indirect influence of phenylephrine on the release of endothelium-derived vasodilators in rat small mesenteric artery. Br J Pharmacol 129:381–387

Eichhorn B, Muller G, Leuner A, Sawamura T, Ravens U, Morawietz H (2009) Impaired vascular function in small resistance arteries of LOX-1 overexpressing mice on high-fat diet. Cardiovasc Res 82:493–502

Erdos B, Kirichenko N, Whidden M, Basgut B, Woods M, Cudykier I, Tawil R, Scarpace PJ, Tumer N (2011) Effect of age on high-fat diet-induced hypertension. Am J Physiol Heart Circ Physiol 301:H164–H172

Fenton M, Huang HL, Hong Y, Hawe E, Kurz DJ, Erusalimsky JD (2004) Early atherogenesis in senescence-accelerated mice. Exp Gerontol 39:115–122

Ferrini MG, Davila HH, Valente EG, Gonzalez-Cadavid NF, Rajfer J (2004) Aging-related induction of inducible nitric oxide synthase is vasculo-protective to the arterial media. Cardiovasc Res 61:796–805

Gómez-Jiménez J, Salgado A, Mourelle M, Martín MC, Segura RM, Peracaula R, Moncada S (1995) L-arginine: nitric oxide pathway in endotoxemia and human septic shock. Crit Care Med 23:253–258

Hamilton CA, Brosnan MJ, Al-Benna S, Berg G, Dominiczak AF (2002) NAD(P)H oxidase inhibition improves endothelial function in rat and human blood vessels. Hypertension 40:755–762

Han J, Hosokawa M, Umezawa M, Yagi H, Matsushita T, Higuchi K, Takeda T (1998) Age-related changes in blood pressure in the senescence-accelerated mouse (SAM): aged SAMP1 mice manifest hypertensive vascular disease. Lab Anim Sci 48:256–263

Hausman N, Martin J, Taggart MJ, Austin C (2011) Age-related changes in the contractile and passive arterial properties of murine mesenteric small arteries are altered by caveolin-1 knockout. J Cell Mol Med. doi:10.1111/j.1582-4934.2011.01457.x

Hermes-Lima M, Willmore WG, Storey KB (1995) Quantification of lipid peroxidation in tissue extracts based on Fe (III)xylenol orange complex formation. Free Radic Biol Med 19:271–280

Herrera MD, Mingorance C, Rodríguez-Rodríguez R, Alvarez de Sotomayor M (2010) Endothelial dysfunction and aging: an update. Ageing Res Rev 9:142–152

Hollenberg SM, Broussard M, Osman J, Parrillo JE (2000) Increased microvascular reactivity and improved mortality in septic mice lacking inducible nitric oxide synthase. Circ Res 86:774–778

Hubert HB, Feinleib M, McNamara PM, Castelli WP (1983) Obesity as an independent risk factor for cardiovascular disease: a 26-year follow-up of participants in the Framingham Heart Study. Circulation 67:968–977

Jiménez-Altayó F, Caracuel L, Pérez-Asensio FJ, Martínez-Revelles S, Messeguer A, Planas AM, Vila E (2009) Participation of oxidative stress on rat middle cerebral artery changes induced by focal cerebral ischemia: beneficial effects of 3,4-dihydro-6-hydroxy-7-methoxy-2,2-dimethyl-1(2H)-benzopyran (CR-6). J Pharmacol Exp Ther 331:429–436

Kannel WB, D'Agostino RB, Cobb JL (1996) Effect of weight on cardiovascular disease. Am J Clin Nutr 63:419S–422S

Kobayasi R, Akamine EH, Davel AP, Rodrigues MA, Carvalho CR, Rossoni LV (2010) Oxidative stress and inflammatory mediators contribute to endothelial dysfunction in high-fat diet-induced obesity in mice. J Hypertens 28:2111–2119

Lauzier B, Delemasure S, Debin R, Collin B, Sicard P, Acar N, Bretillon L, Joffre C, Bron A, Creuzot-Garcher C, Vergely C, Rochette L (2008) Beneficial effects of myocardial postconditioning are associated with reduced oxidative stress in a senescent mouse model. Transplantation 85:1802–1808

Lloréns S, de Mera RM, Pascual A, Prieto-Martín A, Mendizábal Y, de Cabo C, Nava E, Jordán J (2007) The senescence-accelerated mouse (SAM-P8) as a model for the study of vascular functional alterations during aging. Biogerontology 8:663–672

Marín J, Rodriguez-Martínez MA (1999) Age-related changes in vascular responses. Exp Gerontol 34:503–512

Márquez-Martín A, Jiménez-Altayó F, Dantas AP, Caracuel L, Planas AM, Vila E (2012) Middle cerebral artery alterations in a rat chronic hypoperfusion model. J Appl Physiol 112:511–518

Martínez-Revelles S, Caracuel L, Márquez-Martín A, Dantas AP, Oliver E, D'Ocon P, Vila E (2012) Increased endothelin-1 vasoconstriction in mesenteric resistance arteries after superior mesenteric ischemia-reperfusion. Br J Pharmacol 165:937–950

Matsumoto T, Sato A, Suenaga H, Kobayashi T, Kamata K (2004) Modulation of shear stress-induced contractile responses and agonist-induced vasodilation in hypercholesterolemic rats. Atherosclerosis 175:31–38

Matsumoto T, Miyamori K, Kobayashi T, Kamata K (2006) Apocynin normalizes hyperreactivity to phenylephrine in mesenteric arteries from cholesterol-fed mice by improving endothelium-derived hyperpolarizing factor response. Free Radic Biol Med 41:1289–1303

Matz RL, de Sotomayor MA, Schott C, Stoclet JC, Andriantsitohaina R (2000) Vascular bed heterogeneity in age-related endothelial dysfunction with respect to NO and eicosanoids. Br J Pharmacol 131:303–311

Moncada S, Higgs EA (2006) The discovery of nitric oxide and its role in vascular biology. Br J Pharmacol 147:S193–S201

Morishita T, Tsutsui M, Shimokawa H, Horiuchi M, Tanimoto A, Suda O, Tasaki H, Huang PL, Sasaguri Y, Yanagihara N, Nakashima Y (2002) Vasculoprotective roles of neuronal nitric oxide synthase. FASEB J 16:1994–1996

Mundy AL, Haas E, Bhattacharya I, Widmer CC, Kretz M, Hofmann-Lehmann R, Minotti R, Barton M (2007) Fat intake modifies vascular responsiveness and receptor expression of vasoconstrictors: implications for diet-induced obesity. Cardiovasc Res 73:368–375

Nakamura H, Izumiyama N, Nakamura K, Ohtsubo K (1989) Age-associated ultrastructural changes in the aortic intima of rats with diet-induced hypercholesterolemia. Atherosclerosis 79:101–111

Novella S, Dantas AP, Segarra G, Novensà L, Bueno C, Heras M, Hermenegildo C, Medina P (2010) Gathering of aging and estrogen withdrawal in vascular dysfunction of senescent accelerated mice. Exp Gerontol 45:868–874

Novella S, Dantas AP, Segarra G, Novensa L, Heras M, Hermenegildo C, Medina P (2011) Aging enhances contraction to thromboxane A(2) in aorta from female senescence-accelerated mice. Age (Dordr). doi:10.1007/s113570119337

Novensa L, Selent J, Pastor M, Sandberg K, Heras M, Dantas AP (2010) Equine estrogens impair nitric oxide production and endothelial nitric oxide synthase transcription in human endothelial cells compared with the natural 17{beta}-estradiol. Hypertension 56:405–411

Piech A, Dessy C, Havaux X, Feron O, Balligand JL (2003) Differential regulation of nitric oxide synthases and their allosteric regulators in heart and vessels of hypertensive rats. Cardiovasc Res 57:456–467

Rask-Madsen C, King GL (2007) Mechanisms of disease: endothelial dysfunction in insulin resistance and diabetes. Nat Clin Pract Endocrinol Metabol 3:46–56

Reilly JJ, Kelly J (2011) Long-term impact of overweight and obesity in childhood and adolescence on morbidity and premature mortality in adulthood: systematic review. Int J Obes (Lond) 35:891–898

Rodriguez WE, Tyagi N, Joshua IG, Passmore JC, Fleming JT, Falcone JC, Tyagi SC (2006) Pioglitazone mitigates renal glomerular vascular changes in high-fat, high-calorie-induced type 2 diabetes mellitus. Am J Physiol Renal Physiol 291:F694–F701

Sinaiko AR, Donahue RP, Jacobs DR Jr, Prineas RJ (1999) Relation of weight and rate of increase in weight during childhood and adolescence to body size, blood pressure, fasting insulin, and lipids in young adults. The Minneapolis Children's Blood Pressure Study. Circulation 99:1471–1476

Spagnoli LG, Orlandi A, Mauriello A, Santeusanio G, de Angelis C, Lucreziotti R, Ramacci MT (1991) Aging and atherosclerosis in the rabbit. 1. Distribution, prevalence and morphology of atherosclerotic lesions. Atherosclerosis 89:11–24

Stewart KG, Zhang Y, Davidge ST (2000) Aging increases PGHS-2-dependent vasoconstriction in rat mesenteric arteries. Hypertension 35:1242–1247

Syyong HT, Chung AW, Yang HH, van Breemen C (2009) Dysfunction of endothelial and smooth muscle cells in small arteries of a mouse model of Marfan syndrome. Br J Pharmacol 158:1597–1608

Takeda T, Hosokawa M, Takeshita S, Irino M, Higuchi K, Matsushita T, Tomita Y, Yasuhira K, Hamamoto H, Shimizu K, Ishii M, Yamamuro T (1981) A new murine model of accelerated senescence. Mech Ageing Dev 17:183–194

Traupe T, Lang M, Goettsch W, Munter K, Morawietz H, Vetter W, Barton M (2002) Obesity increases prostanoid-mediated vasoconstriction and vascular thromboxane receptor gene expression. J Hypertens 20:2239–2245

Ungvari Z, Buffenstein R, Austad SN, Podlutsky A, Kaley G, Csiszar A (2008) Oxidative stress in vascular senescence: lessons from successfully aging species. Front Biosci 13:5056–5070

Ungvari Z, Bagi Z, Feher A, Recchia FA, Sonntag WE, Pearson K, de Cabo R, Csiszar A (2010) Resveratrol confers endothelial protection via activation of the antioxidant transcription factor Nrf2. Am J Physiol Heart Circ Physiol 299: H18–H24

Van der Loo B, Labugger R, Skepper JN, Bachschmid M, Kilo J, Powell JM, Palacios-Callender M, Erusalimsky JD, Quaschning T, Malinski T, Gygi D, Ullrich V, Luscher TF (2000) Enhanced peroxynitrite formation is associated with vascular aging. J Exp Med 192:1731–1744

Van Guilder GP, Westby CM, Greiner JJ, Stauffer BL, DeSouza CA (2007) Endothelin-1 vasoconstrictor tone increases with age in healthy men but can be reduced by regular aerobic exercise. Hypertension 50:403–409

Vila E, Salaices M (2005) Cytokines and vascular reactivity in resistance arteries. Am J Physiol Heart Circ Physiol 288: H1016–H1021

Yagi K, Komura S, Sasaguri Y, Yoshino K, Ohishi N (1995) Atherogenic change in the thoracic aorta of the senescence-accelerated mouse. Atherosclerosis 118:233–236

Yang YM, Huang A, Kaley G, Sun D (2009) eNOS uncoupling and endothelial dysfunction in aged vessels. Am J Physiol Heart Circ Physiol 297:H1829–H1836

Yogo K, Shimokawa H, Funakoshi H, Kandabashi T, Miyata K, Okamoto S, Egashira K, Huang P, Akaike T, Takeshita A (2000) Different vasculoprotective roles of NO synthase isoforms in vascular lesion formation in mice. Arterioscler Thromb Vasc Biol 20:E96–E100

Zanetti M, Gortan Cappellari G, Burekovic I, Barazzoni R, Stebel M, Guarnieri G (2010) Caloric restriction improves endothelial dysfunction during vascular aging: effects on nitric oxide synthase isoforms and oxidative stress in rat aorta. Exp Gerontol 45:848–855

Zhu BH, Ueno M, Matsushita T, Fujisawa H, Seriu N, Nishikawa T, Nishimura Y, Hosokawa M (2001) Effects of aging and blood pressure on the structure of the thoracic aorta in SAM mice: a model of age-associated degenerative vascular changes. Exp Gerontol 36:111–124